SYNTHESIS AND CHARACTERIZATION OF CERAMIC COMPOSITES

By

Amit K. Shrestha

A Research Paper

Submitted in Partial Fulfillment of the

Requirements for the

Master of Science Degree

In

Management Technology

Approved: 3 Semester Credits

Rajiv Asthana

Dr. Rajiv Asthana

Research Advisor

The Graduate School

University of Wisconsin-Stout

May, 2006

The Graduate School

University of Wisconsin-Stout

Menomonie, WI 54751

ABSTRACT

	Shrestha	Amit	K
(Writer)	(Last Name)	(First Name)	(Middle Initial)

Synthesis and Characterization of Ceramic Composites

(Title)

Management Technology	Dr. Rajiv Asthana	May, 2006	56
(Graduate Program)	(Research Advisor)	(Month/Year)	(# of Pages)

American Psychological Association, 5th edition

(Name of Style Manual Used in This Study)

Due to inherent brittleness, ceramic materials have limited use in industrial applications, especially in structural components at high temperatures where they can outperform other material classes. By adding a small amount of a metal, ceramics can be imparted some toughness at little expense to their other useful engineering properties. Aluminum oxide is the most widely used and characterized ceramic material. In this research, aluminum oxide was used as the ceramic matrix material and a two-step powder metallurgy approach involving powder compaction and sintering approach was implemented to synthesize the aluminum oxide-bronze composites. The sintered composites were characterized for density, porosity, hardness, and fracture strength as a function of the material composition and sintering parameters.

ACKNOWLEDGEMENTS

I would like to acknowledge my family and friends for their constant support in the pursuit of all my goals. A sincere appreciation is extended to the Department of Engineering and Technology, University of Wisconsin-Stout. A special thanks to my research advisor Dr. Rajiv Asthana who took time to meet with me, guided and supported me in every possible way throughout this research work. Words of gratitude will not be enough for him.

There are many who helped me from behind the scenes – my sincere thanks to Dr. Tom Lacksonen, Dr. John Dzissah and Dr. Mehar Arora. Here, I would like to thank everyone who supported me in completing this research work.

TABLE OF CONTENTS

LIST OF TABLES

LIST OF FIGURES

Chapter I: Introduction

Ceramic materials are inorganic and non-metallic; however they may contain both metallic and nonmetallic elements. This class of materials includes both traditional ceramics such as clay, tile, porcelain, and glass, as well as modern technical ceramics such as carbides, borides, oxides, and nitrides of various elements, which are used in high-technology applications. Examples of technical ceramics include aluminum oxide, aluminum nitride, boron carbide, boron nitride, silicon carbide, titanium diboride, silicon nitride, sialons, zirconium dioxide, barium titanate, and ceramic superconductors. Usually, ceramics attain their properties during a sintering process at high temperatures.

As monolithic polycrystalline materials, ceramics exhibit low toughness but high stiffness (i.e., high elastic modulus). Generally stronger under compression than under tension, ceramics are poor conductors of heat and electricity. Ceramics are lightweight ionic compounds with high atomic bond energies, which leads to high melting points (Kingery, 1976).

Problem Statement

To synthesize and characterize new ceramic composites with improved toughening potential while studying the effects of the volume fraction of metal powder, compaction pressure, sintering temperature, and sintering time on density, porosity, fracture strength and hardness.

An Overview of the Study

In spite of their superior heat-resistance, wear-resistance, durability, strength, hardness, and corrosion resistance, monolithic ceramics are inherently brittle and less forgiving than metals to surface and internal flaws, which limits their use in industrial applications, especially in structural components at high temperatures where they can outperform other material classes.

One method to overcome the low toughness of ceramics is to increase the misorientation between grains to hinder crack propagation across the grain boundaries. Another method introduces tiny microcracks in noncubic crystalline ceramics (Al_2O_3, TiO_2, etc.) in order to increase the fracture energy, and therefore the toughness. These subcritical microscopic cracks provide an additional mechanism to dissipate the energy although they also tend to decrease the strength. Yet another method to toughen ceramics is based on the beneficial role of sintering aids that are frequently added to ceramics to stimulate sintering. Sintering aids often form compounds that constantly deflect cracks during the latter's growth, thus requiring increased energy consumption for crack propagation.

Combining two or more ceramics such as SiC whiskers reinforcedAl_2O_3 is yet another method to toughen ceramics. Considerable toughness gains are possible; for example, Al_2O_3 containing SiC whiskers nearly doubles the fracture toughness of alumina. The whiskers inhibit crack advance and absorb energy when they are pulled out or fractured by a propagating crack. The interface strength between different ceramics in such materials must be carefully tailored; too high a bond strength will impart poor toughness because of limited fiber pullout, and too low a strength will consume little energy during pullout, with negligible gains in toughness. The whiskers should be thermally and chemically stable at processing and service temperatures.

An interesting approach to enhance the toughness of ceramics is to use the energy of propagating cracks to trigger a solid-state phase change in the vicinity of the crack in such a way that volume changes on transformation accommodate the stresses to inhibit the growth of crack. This approach is called transformation toughening, and the classic example of this mode of toughening is yttria-stabilized zirconia. In transformation toughened zirconia ceramics, fine particles of partially stabilized ZrO_2 are dispersed within an Al_2O_3 or a ZrO_2 matrix. Small quantities (2–4%) of oxides such as MgO, Y_2O_3, and CaO are added to ZrO_2 and equilibrated at ~1100°C to form a phase with a tetragonal crystal structure. The oxide phase stabilizes the tetragonal structure. The material is then cooled rapidly to room temperature to prevent the transformation of the tetragonal phase into the more stable monoclinic form (the transformation kinetics for this reaction are rather sluggish). This stabilizes the metastable tetragonal ZrO_2 phase at room temperature rather than the more stable monoclinic phase. The stress field at the tip of an advancing crack causes the tetragonal ZrO_2 to transform into the stable monoclinic phase accompanied by a slight (~2%) volume expansion of transformed particles. This expansion of the dispersed ZrO_2 particles results in a compressive stress on the crack tip that arrests the latter's growth, thus imparting toughness to the ceramic.

Toughness can be enhanced and cracks can be blunted by distributing a soft, plastically deformable phase in a ceramic matrix which is the basis of a class of materials called cermets (e.g., Co binder in WC). Cermets contain fine (0.5–10 μm) grains of a hard carbide (WC or TaC) bonded with a thin (0.5–1 μm) layer of a metallic binder such as cobalt, which partially dissolves the carbide grains and forms a strong chemical bond to it. Cermets may also contain fine grains of two carbides; for example, WC intermixed with TaC and TiC grains. These latter carbides stabilize the tungsten carbide and reduce the erosion during machining. Ceramic-matrix composites containing a small amount of a ductile metal phase possess good toughness.

Purpose of the study

The purpose of this study was to synthesize new ceramic composites with toughening potential by adding varying proportions of a ductile metal powder in the primary ceramic matrix material, which was aluminum oxide (γ-phase). The ductile metal powder used as the dispersed second phase in Al_2O_3 was 70-30 bronze (70% Cu – 30% Zn). Copper is known to bond strongly to alumina ceramics, but is quite soft in a pure state. It is also known that Cu-O alloys strongly adhere to alumina, which suggests that sintering of the composites could be carried out under ambient conditions without the need of vacuum. In order to achieve toughening without extensive loss of strength, bronze powder instead of pure Cu was used. The effects of the volume fraction of metal powder, compaction pressure, sintering temperature, and sintering time on density, porosity, fracture strength and hardness were studied.

Research approach

A conventional powder blending, compaction and sintering methodology was implemented for the synthesis of the ceramic-metal composites. Coarse nanometer-size aluminum oxide powder was selected as the primary matrix material. Varying proportions (0-20%) of the bronze powders were added to Al_2O_3 powder, mechanically mixed, and pressed in a hydraulic press to form disc-shaped compacts that were sintered in air in a programmable furnace under different conditions of time and temperature. The sintered composites were characterized for density, porosity, hardness, and fracture strength as a function of the material composition and sintering parameters. The experimental data were systematically recorded and analyzed to evaluate mechanical behavior of the synthesized materials.

Significance of the Study

As stated in a preceding paragraph, this research implemented a materials design approach to overcome the inherent lack of toughness of brittle ceramics. This approach involved judicious selection of ceramic and metal powders to synthesize ceramic-matrix composites via a classical powder metallurgy technique, followed by preliminary physical and mechanical characterization of the composite. The research outcomes provide experimental data and insight into processing and properties of the fabricated composites.

Chapter II: Literature Review

Several different approaches have been used to impart toughness to industrial ceramics. Some of these approaches were mentioned in Chapter I, which include: increasing the misorientation between grains to hinder crack propagation across the grain boundaries, introducing microcracks in ceramics such as Al_2O_3 and TiO_2 to dissipate the fracture energy, incorporating suitable sintering aids that form compounds that deflect cracks during the latter's growth, combining two or more ceramics such as SiC whiskers and Al_2O_3, transformation toughening in which volume changes accompanying a crystalline phase transformation accommodate the stresses at crack tip, and crack impeding by dispersing plastically deformable particles or fibers in a brittle ceramic. In this case, crack is either arrested or bows out.

By adding a small amount of a ductile metallic phase, ceramics can be imparted toughness at little expense to their other useful engineering properties. Ceramic composites containing fine metal dispersions can be prepared using powder metallurgy. For example, silicon carbide ceramics containing up to 24.6 vol% dispersed TiC particles yielded fully dense composites by hot-pressing at 2000°C with 1 wt% Al and 1 wt% C added (Wei and Becher, 1984). It was observed that at high temperatures, the fracture strength of SiC hot pressed with Al and C additives was improved by the addition of TiC particles.

The improvement in the toughness of brittle ceramics through metal dispersions is attractive because of extremely high concentration of internal interfaces that become available for energy dissipation during loading. Similar practices have been applied in dielectric matrices. Particle dispersions in dielectric matrices have been produced; for example, semiconductor or metal dispersions in glass have been developed for applications in optoelectronic devices, and magnetic, and solar energy conversion devices.

Metal composites containing dispersions of ceramic particles also have been designed and fabricated. The goal here is to enhance the strength of the metal even at some expense to toughening. Powder metallurgy has been used to synthesize metal-based composites containing ceramics. Generally, such materials are fabricated using high-energy ball milling followed by hot consolidation. For example, creep-resistant, lightweight Mg/SiC nanocomposites have been obtained by using milling and hot extrusion (Ferkel & Mordike, 2001). The Ultimate Tensile Strength (UTS) of the hot extruded composite doubled as compared to un-reinforced Mg. Even a low volume fraction of SiC nanoparticles when dispersed in pure Mg significantly increased the strength and, in particular, the creep resistance of the material. Metal-matrix composites (MMCs) containing micrometer-scale reinforcements such as continuous-fiber reinforced B/Al, C/Al, and C/Mg, and SiC/Al are already in use. In addition, low-cost discontinuous metal composites such as $C_{(p)}$Al, $Al_2O_{3(p)}$/Al, $SiC_{(p)}$/Al, microballoon/Al, and fly ash/Al have been synthesized for potential automotive and other industrial applications. works.

Recent research to synthesize tough ceramics by dispersing a metallic phase, and strong metals by dispersing a ceramic phase have employed nanoscale dispersions. For example, mechanical properties of Cu-matrix composites reinforced by carbon nanotubes (CNT) were investigated by Dong et al (2001). These composites were synthesized using a hot pressing technique with 350 MPa pressure and 850°C temperature. A decrease in the composite's coefficient of friction and low wear losses characterized the composites.

A variety of other novel nano-ceramics and ceramic- and metal nanocomposites have been synthesized. These materials have been processed using high-energy ball milling, internal oxidation, hot consolidation, crystallization of amorphous solid, sol-gel processing, and vapor-phase and vapor-liquid-solid deposition. Ceramic nanocomposites possessing improved fracture toughness include hot-pressed composites of CNT/SiC, Al_2O_3/SiC, MgO/SiC, W/Al_2O_3, Al_2O_3/Co, ZrO_2/Ni and Si_3N_4/SiC. The powders are first synthesized using chemical reactions and precipitation. The resulting material is then reduced by hydrogen and hot press sintered at high temperatures and pressures to produce nanocomposites. Considerable improvements in mechanical strength, hardness and fracture toughness are achieved.

Creep-resistant dispersion-strengthened (DS) composites such as Cu/Al_2O_3 have been used in the aerospace industry for nearly forty years. These composites contain fine dispersions (10-100 nm) and low volume fractions (10-15%) of ceramic oxide particles in a high-temperature alloy, usually Ni-base. The dispersed oxide phase primarily serves as a barrier to the motion of dislocations rather than as the load bearing constituent. The attractive feature of the DS composite is its ability to retain high yield strength, creep resistance, and oxidation resistance at elevated temperatures rather than an ability to enhance the room-temperature yield strength (Ying & Zhang, 2000). The thrust of the current research on ceramics is to improve the room-temperature toughness of brittle ceramics through fine metal dispersions or other means.

Chapter III: Methodology

Material selection and description

As discussed in the preceding chapters, toughening of ceramics is a topic of contemporary interest in the research and development of advanced materials. Aluminum oxide is the most widely used and characterized ceramic material. Hence, in this research, aluminum oxide was used as the ceramic matrix material. Nanometer-size aluminum oxide (Al_2O_3) powder was obtained from Reynold's Metals Co.

Research Methodology

A two-step powder metallurgy approach involving powder compaction and sintering was implemented to synthesize the aluminum oxide-bronze composites. The powder metallurgy technique to fabricate the composites consisted of the following steps:

(1) The aluminum oxide powder was hand mixed with different fractions of bronze (70% Cu, 30% Zn) powder using basic laboratory tools.

(2) Pure aluminum oxide powder (with 0% Bronze) was compacted under a pressure of 20,000 lb to prepare 27 disc-shaped samples (3 groups of 9 samples for sintering at 3 different temperatures of 1300°C, 1400°C, and 1500°C).

(3) The aluminum oxide powders containing 5%, 10% and 20% by weight of Bronze powder were compacted under a pressure of 20,000 lb to prepare 54 disc-shaped samples (3 groups of 18 samples). In each group 18 samples were further divided into 3 subgroups for sintering at 3 different temperatures; 1300°C, 1400°C, 1500°C.

(4) The pure aluminum oxide powder (with 0% weight Bronze) compacts were sintered for 0.5hr, 2hr and 4hr at temperatures of 1300°C, 1400°C and 1500°C, with 3 samples for each time/temperature combination. The experiments were conducted under normal ambient atmosphere.

(5) The aluminum oxide powder compacts (with 5%, 10% and 20% weight Bronze) were sintered for 0.5hr, 2hr and 4hr at temperatures of 1300°C, 1400°C and 1500°C, with 2 samples for each time/temperature combination. The experiments were conducted under normal ambient atmosphere.

(6) The sintered coupons were characterized for density from weight and volume measurements. For samples that had cracked, and presented difficulty in measuring the bulk dimensions, a water displacement method was employed to determine the coupon volume. From the measured density data, porosity content in each sintered coupon was calculated.

(7) The samples were tested for modulus of rupture (MOR) using a three-point bend test fixture.

(8) Selected samples were sectioned on a low-speed diamond saw to determine the rate of cutting as mm^2/s. The cutting speed was maintained constant at 200 revolutions per minute.

Instrumentation

All the equipment required for the research was available in the Ceramics and Powder Metallurgy Laboratory of the Department of Engineering and Technology at UW-Stout. The major tools and equipment used to accomplish this research were:

hydraulic press for powder compaction, tool steel punches and dies, programmable sintering furnace, low-speed diamond saw, electronic balance, calipers, a desktop three-point bend test fixture for determining the modulus of rupture (flexural strength), and other accessory. Ceramic carrier boats for sintering and die lubricant (zinc stearate) were also used.

Analysis

This research was designed to yield the following technical information:

(1) The effect of sintering temperature on part density and porosity of monolithic alumina and alumina-bronze composites with different bronze content.

(2) The effect of sintering time on part density and porosity of monolithic alumina and alumina-bronze composites with different bronze content.

(3) The modulus of rupture (MOR) for both monolithic alumina and alumina-bronze composites containing different percentages of bronze.

(4) The cutting rate (as m^2/s) as an indirect measure of the hardness of the test coupons.

Chapter IV: Results and discussion

Density and porosity

Tables 1A through 12A summarize the measured density and estimated porosity of press and sintered aluminum oxide based composite specimens containing 5%, 10% and 20% weight Bronze fabricated from the green state under an external force of 20,000lb. The tables also provide the density of pure aluminum oxide composites (with 0% weight Bronze) that were sintered for 0.5hr, 2hr and 4hr at 1300°C, 1400°C and 1500°C, with 3 samples for each time-temperature combination. In addition, the preceding tables present density of the aluminum oxide compacts (with 5%, 10% and 20% weight Bronze) that were sintered for 0.5hr, 2hr and 4hr at 1300°C, 1400°C and 1500°C with 2 samples for each time-temperature combination.

The theoretical density of aluminum oxide composites with 0%, 5%, 10% and 20% weight fraction of bronze were calculated using the equation (I) given below.

$$d_{Comp} = d_{Al_2O_3}(1 - Ø_{Al_2O_3}) + d_{Bronze} * Ø_{Bronze} \quad \text{----------------} \quad I$$

where,

d_{Comp} = Theoretical density of compacted composite

$d_{Al_2O_3}$ = Theoretical density of Al_2O_3 = 3900 kg/m^3

$Ø_{Al_2O_3}$ = Volume fraction of Al_2O_3 in the composite

d_{Bronze} = Theoretical density of bronze (70%Cu-30%Zn) = 8530 kg/m^3

$^{\varnothing}_{Bronze}$ = Volume fraction of bronze in the composite

The volume fraction of bronze in the composites was calculated from the measured weight fraction using the equation (II) given below:

$$^{W}_{Bronze} = {^{\varnothing}_{Bronze}} \Big/ \left[{^{\varnothing}_{Bronze}} + (1 - {^{\varnothing}_{Bronze}}) * {^{d}_{Al_2O_3}} \Big/ {^{d}_{Bronze}} \right] \text{ ---- II}$$

where,

$^{W}_{Bronze}$ = Weight fraction of bronze in the composite

$^{\varnothing}_{Bronze}$ = Volume fraction of bronze in the composite

The Rule-of-mixture (ROM) method was applied to calculate the theoretical densities for the Al_2O_3 – Bronze composite compacts as shown in Table 13.

After calculating the theoretical and experimental density values, the porosity content in all the Al_2O_3 – Bronze composites sintered under different time and temperature conditions were determined using the formula given below:

$$\% \text{ Porosity} = \left[(\text{Theoretical density - Experimental density}) * 100\right] \Big/ \text{Theoretical density}$$

Tables 1A through 12A also summarize the estimated porosity for the compacted aluminum oxide powders with 0%, 5%, 10% and 20% weight Bronze. Tables 14 through 16 provide data to compare sintered density and %Bronze of Al_2O_3 – Bronze composite at 1300°C, 1400°C and 1500°C sintering temperatures for 0.5hr, 2.0hr and 4.0hr. Tables 17 through 19 provide data to compare sintering temperature and sintered density of Al_2O_3 – Bronze composite with 0%, 5%, 10% and 20% weight bronze for 0.5hr, 2.0hr and 4.0hr. Similarly Table 20 through 23 provide data to compare sintering time and sintered density of Al_2O_3 – Bronze composite at sintering temperatures 1300°C, 1400°C and 1500°C with 0%, 5%, 10% and 20% bronze.

MOR and cutting rate

A three-point bend test was performed on forty-nine Al_2O_3 – Bronze composite samples to calculate modulus of rupture (MOR). On the three-point bend test fixture, each division on the deflection dial gage represents 7lb force. Thus, by measuring the deflection to fracture, the fracture force could be estimated from which the MOR value is obtained using the formula:

$$\sigma = F*L / \Pi (R)^3 \quad \text{------------------} \quad III$$

where,

σ = MOR(Modulus of Rupture) / Flexural strength / Rupture strength

F = Force in Newton

L = Spacing between the two supports on the test fixture = 1.4cm = 14mm

R = Radius of the specimen

Only approximate values of the MOR were obtained because the press-and-sintered coupons were essentially non-standard and only roughly satisfied the assumptions of equation (III).

A test to determine the cutting rate was performed on thirty Al_2O_3 – Bronze composite samples using a low-speed diamond saw at a constant cutting speed of 200 revolutions per minute. The cutting test results were expressed as area cut per unit time.

Table 1B through 12B provide estimated modulus of rupture (MOR) and cutting rate of Al_2O_3 – Bronze composite with 0%, 5%, 10% and 20% Bronze under sintering temperatures 1300°C, 1400°C and 1500°C. Table 24 provides a consolidated data on sintered density, porosity, MOR and cutting rate of Al_2O_3 – Bronze composite with 0%, 5%, 10% and 20% Bronze under sintering temperatures 1300°C, 1400°C and 1500°C.

Figure 1 shows a negative correlation between % porosity and MOR. As the % Porosity of Al_2O_3 – Bronze composite increases, the MOR decreases. This result is consistent with the theoretical behavior which predicts a weakening of the ceramic composites with increasing defect content. Figure 2 reflects a positive correlation between % Bronze and % porosity in the Al_2O_3 – Bronze composite. With increasing % Bronze in the composite, the % porosity increases. This behavior is inconsistent with the theoretical expectations. Bronze, being a heavier alloy than monolithic alumina, should cause an increase in the composite density at increasing bronze contents. The reverse trend observed in Fig. 2 is a consequence of the void and crack formation in the composite specimens, which led to inaccurate measurements of volume for density and porosity estimation. Finally, Fig. 3 shows a positive correlation between % Bronze and the cutting rate for the Al_2O_3 – Bronze composite compacts. It shows that the cutting rate increases as the bronze content in the Al_2O_3 – bronze composite increases. Bronze would cause some softening in the alumina compact which should essentially reduce the cutting rate. However, as the sintering experiments were conducted in air, oxidation of bronze constituents is a strong likelihood. Thus, formation of copper oxides and zinc oxides will be unavoidable, and these oxides will essentially enhance the effective hardness and the cutting rate.

Limitations of the study

(1) The experimental research was limited to Al_2O_3 – Bronze (70%Cu-30%Zn) composites and only a limited number of composite samples could be synthesized due to both cost and time constraints. Nevertheless, the experimental results provided a preliminary assessment of the effect of air sintering of bronze-alumina composites on some physical and mechanical characteristics.

(2) Experimental error in measuring the dimensions of the compacts could not be avoided due to the cracks formed in the samples after sintering at elevated temperatures. Whereas a water displacement method was used to estimate the sample volume for use in the density and porosity calculations for samples that displayed visible surface cracking, the use of two different methods of volume measurements, and the possibility of internal voids and cracks not visible at the specimen surface possibly led to errors in measurements.

Suggestions for future work

The cracking of samples led to errors and inconsistencies in the experimental measurements. The problem was caused due to melting and accompanying expansion of the bronze powders even below the lowest sintering temperature of 1300° C used in the present study. This volumetric expansion upon phase change caused internal stresses and cracks to develop even before the alumina powders developed 'necks' via thermally-induced atomic mass transport processes. In addition, zinc vapor formation at high sintering temperatures could cause internal gas pressure to build, leading to void formation and cracking. During cooling at the conclusion of sintering, the liquid bronze would resolidify, leading to internal shrinkage and shrinkage porosity to form. These changes will lead to defect formation and eventual weakening of the composite test samples. It is recommended that a two-step press and sinter technique is not viable to synthesize these composites. Instead, hot pressing should be used where compaction and sintering take place concurrently under large hydrostatic pressures which reduce crack and void formation.

Table 1A

Sintered Density and % Porosity of Al_2O_3 – Bronze Composite (0% Bronze; Sintering Temperature = 1300°C)

Sample	Sintering	After Sintering												
Number	Time (Hrs.)	Weight (gm)	Weight (kg)	Diameter (Inches)	Diameter (m)	Radius (m)	Thickness (Inches)	Thickness (m)	Volume (cm^3)	Volume (m^3)	Density (kg/m^3)	Average Density (kg/m^3)	Porosity (%)	Average Porosity (%)
1	0.5	11.25	0.0113	1.0055	0.0255	0.0128	0.2680	0.0068		3.49E-06	3225.98		17.2826	
2	0.5	10.98	0.0110	1.0070	0.0256	0.0128	0.2625	0.0067		3.43E-06	3204.96	3191.09	17.8216	18.18
3	0.5	11.07	0.0111	1.0125	0.0257	0.0129	0.2670	0.0068		3.52E-06	3142.35		19.4270	
4	2	11.28	0.0113	0.9875	0.0251	0.0125	0.2640	0.0067		3.31E-06	3404.39		12.7080	
5	2	11.19	0.0112	0.9875	0.0251	0.0125	0.2650	0.0067		3.33E-06	3364.48	3507.40	13.7313	10.07
6	2	11.26	0.0113	0.9910	0.0252	0.0126	0.3000	0.0076	3.00	0.000003	3753.33		3.7607	
7	4	11.27	0.0113	0.9795	0.0249	0.0124	0.2615	0.0066		3.23E-06	3490.21		10.5075	
8	4	11.20	0.0112	0.9780	0.0248	0.0124	0.2605	0.0066		3.21E-06	3492.53	3497.11	10.4479	10.33
9	4	11.24	0.0112	0.9775	0.0248	0.0124	0.2605	0.0066		3.2E-06	3508.59		10.0361	

Table 2A

Sintered Density and % Porosity of Al_2O_3 – Bronze Composite (0% Bronze; Sintering Temperature = 1400°C)

Sample	Sintering	After Sintering											
Number	Time (Hrs.)	Weight (gm)	Weight (kg)	Diameter (Inches)	Diameter (m)	Radius (m)	Thickness (Inches)	Thickness (m)	Volume (m^3)	Density (kg/m^3)	Average Density (kg/m^3)	Porosity (%)	Average Porosity (%)
1	0.5	11.10	0.0111	0.9605	0.0244	0.0122	0.2550	0.0065	3.03E-06	3666.03		5.9992	
2	0.5	11.16	0.0112	0.9590	0.0244	0.0122	0.2530	0.0064	2.99E-06	3726.61	3683.26	4.4458	5.56
3	0.5	11.18	0.0112	0.9595	0.0244	0.0122	0.2580	0.0066	3.06E-06	3657.13		6.2275	
4	2	11.21	0.0112	0.9535	0.0242	0.0121	0.2570	0.0065	3.01E-06	3727.68		4.4184	
5	2	11.06	0.0111	0.9520	0.0242	0.0121	0.2510	0.0064	2.93E-06	3777.60	3747.55	3.1386	3.91
6	2	11.14	0.0111	0.9530	0.0242	0.0121	0.2550	0.0065	2.98E-06	3737.38		4.1698	
7	4	10.96	0.0110	0.9500	0.0241	0.0121	0.2490	0.0063	2.89E-06	3789.41		2.8356	
8	4	11.02	0.0110	0.9495	0.0241	0.0121	0.2510	0.0064	2.91E-06	3783.78	3792.72	2.9800	2.75
9	4	11.17	0.0112	0.9495	0.0241	0.0121	0.2530	0.0064	2.94E-06	3804.97		2.4368	

Table 3A

Sintered Density and % Porosity of Al_2O_3 – Bronze Composite (0% Bronze; Sintering Temperature = 1500°C)

Sample	Sintering	After Sintering											
Number	Time (Hrs.)	Weight (gm)	Weight (kg)	Diameter (Inches)	Diameter (m)	Radius (m)	Thickness (Inches)	Thickness (m)	Volume (m^3)	Density (kg/m^3)	Average Density (kg/m^3)	Porosity (%)	Average Porosity (%)
1	0.5	11.18	0.0112	0.9450	0.0240	0.0120	0.2500	0.0064	2.87E-06	3890.86		0.2342	
2	0.5	11.10	0.0111	0.9450	0.0240	0.0120	0.2500	0.0064	2.87E-06	3863.02	3885.06	0.9481	0.38
3	0.5	11.21	0.0112	0.9450	0.0240	0.0120	0.2500	0.0064	2.87E-06	3901.31		-0.0335	
4	2	11.11	0.0111	0.9450	0.0240	0.0120	0.2525	0.0064	2.9E-06	3828.22		1.8405	
5	2	11.04	0.0110	0.9450	0.0240	0.0120	0.2490	0.0063	2.86E-06	3857.57	3861.53	1.0879	0.99
6	2	11.27	0.0113	0.9450	0.0240	0.0120	0.2515	0.0064	2.89E-06	3898.79		0.0309	
7	4	11.07	0.0111	0.9450	0.0240	0.0120	0.2520	0.0064	2.9E-06	3822.01		1.9998	
8	4	11.01	0.0110	0.9450	0.0240	0.0120	0.2470	0.0063	2.84E-06	3878.24	3842.37	0.5579	1.48
9	4	11.26	0.0113	0.9450	0.0240	0.0120	0.2560	0.0065	2.94E-06	3826.86		1.8753	

Table 4A

Sintered Density and % Porosity of Al_2O_3 – Bronze Composite (5% Bronze; Sintering Temperature = 1300°C)

Sample	Sintering	After Sintering											
Number	Time (Hrs.)	Weight (gm)	Weight (kg)	Diameter (Inches)	Diameter (m)	Radius (m)	Thickness (Inches)	Thickness (m)	Volume (m^3)	Density (kg/m^3)	Average Density (kg/m^3)	Porosity (%)	Average Porosity (%)
1	0.5	10.60	0.0106	1.0300	0.0262	0.0131	0.2575	0.0065	3.52E-06	3014.83	3025.13	24.7798	24.52
2	0.5	10.60	0.0106	1.0295	0.0261	0.0131	0.2560	0.0065	3.49E-06	3035.44		24.2656	
3	2	10.63	0.0106	1.0185	0.0259	0.0129	0.2505	0.0064	3.34E-06	3178.42	3169.08	20.6981	20.93
4	2	10.81	0.0108	1.0180	0.0259	0.0129	0.2565	0.0065	3.42E-06	3159.74		21.1643	
5	4	10.66	0.0107	1.0205	0.0259	0.0130	0.2485	0.0063	3.33E-06	3200.46	3206.47	20.1481	20.00
6	4	10.68	0.0107	1.0175	0.0258	0.0129	0.2495	0.0063	3.32E-06	3212.48		19.8484	

Table 5A

Sintered Density and % Porosity of Al_2O_3 – Bronze Composite (5% Bronze; Sintering Temperature = 1400°C)

Sample Number	Sintering Time (Hrs.)	After Sintering Weight (gm)	Weight (kg)	Diameter (Inches)	Diameter (m)	Radius (m)	Thickness (Inches)	Thickness (m)	Volume (cm^3)	Volume (m^3)	Density (kg/m^3)	Average Density (kg/m^3)	Porosity (%)	Average Porosity (%)
1	0.5	10.49	0.0105	1.0205	0.0259	0.0130	0.2575	0.0065	2.95	2.95E-06	3555.93	3372.54	11.2791	15.85
2	0.5	10.55	0.0106	1.0160	0.0258	0.0129	0.2490	0.0063		3.31E-06	3189.14		20.4306	
3	2	10.60	0.0106	1.0140	0.0258	0.0129	0.2500	0.0064		3.31E-06	3204.04	3177.58	20.0589	20.72
4	2	10.79	0.0108	1.0145	0.0258	0.0129	0.2585	0.0066		3.42E-06	3151.12		21.3793	
5	4	10.66	0.0107	1.0320	0.0262	0.0131	0.2550	0.0065	3.20	3.20E-06	3331.25	3269.53	16.8850	18.42
6	4	10.57	0.0106	1.0140	0.0258	0.0129	0.2490	0.0063		3.30E-06	3207.80		19.9650	

Table 6A

Sintered Density and % Porosity of Al_2O_3 – Bronze Composite (5% Bronze; Sintering Temperature = 1500°C)

Sample	Sintering	After Sintering												
Sample Number	Time (Hrs.)	Weight (gm)	Weight (kg)	Diameter (Inches)	Diameter (m)	Radius (m)	Thickness (Inches)	Thickness (m)	Volume (cm^3)	Volume (m^3)	Density (kg/m^3)	Average Density (kg/m^3)	Porosity (%)	Average Porosity (%)
1	0.5	11.48	0.0115	1.0100	0.0257	0.0128	0.2695	0.0068		3.54E-06	3244.50	3249.78	19.0493	18.92
2	0.5	10.63	0.0106	1.0115	0.0257	0.0128	0.2480	0.0063		3.27E-06	3255.05		18.7862	
3												3576.27		10.77
4	2	10.55	0.0106	1.0310	0.0262	0.0131	0.2530	0.0064	2.95	2.95E-06	3576.27		10.7717	
5	4	10.45	0.0105	1.0250	0.0260	0.0130	0.2550	0.0065	3.00	3.00E-06	3483.33	3327.35	13.0905	16.98
6	4	10.42	0.0104	1.0075	0.0256	0.0128	0.2515	0.0064		3.29E-06	3171.37		20.8739	

Table 7A

Sintered Density and % Porosity of Al_2O_3 – Bronze Composite (10% Bronze; Sintering Temperature = 1300°C)

Sample	Sintering	After Sintering												
Number	Time (Hrs.)	Weight (gm)	Weight (kg)	Diameter (Inches)	Diameter (m)	Radius (m)	Thickness (Inches)	Thickness (m)	Volume (cm^3)	Volume (m^3)	Density (kg/m^3)	Average Density (kg/m^3)	Porosity (%)	Average Porosity (%)
1	0.5	11.38	0.0114	1.0335	0.0263	0.0131	0.2815	0.0072	4.00	4.00E-06	2845.00	2866.80	30.9968	30.47
2	0.5	11.41	0.0114	1.0385	0.0264	0.0132	0.2660	0.0068	3.95	3.95E-06	2888.61		29.9392	
3	2	11.35	0.0114	1.0280	0.0261	0.0131	0.2905	0.0074	3.95	3.95E-06	2873.42	3053.54	30.3076	25.94
4	2	11.38	0.0114	1.0265	0.0261	0.0130	0.2595	0.0066		3.52E-06	3233.66		21.5701	
5	4	11.34	0.0113						3.00	3.00E-06	3780.00	3354.10	8.3192	18.65
6	4	11.42	0.0114	1.0330	0.0262	0.0131	0.2670	0.0068	3.90	3.90E-06	2928.21		28.9788	

Table 8A

Sintered Density and % Porosity of Al_2O_3 – Bronze Composite (10% Bronze; Sintering Temperature = 1400°C)

Sample	Sintering	After Sintering												
Number	Time (Hrs.)	Weight (gm)	Weight (kg)	Diameter (Inches)	Diameter (m)	Radius (m)	Thickness (Inches)	Thickness (m)	Volume (cm^3)	Volume (m^3)	Density (kg/m^3)	Average Density (kg/m^3)	Porosity (%)	Average Porosity (%)
1	0.5	11.29	0.0113	1.0255	0.0260	0.0130	0.2655	0.0067		3.59E-06	3141.71	3183.71	23.8004	22.78
2	0.5	11.29	0.0113	1.0275	0.0261	0.0130	0.2635	0.0067	3.50	3.50E-06	3225.71		21.7629	
3	2	11.21	0.0112	1.0280	0.0261	0.0131	0.2625	0.0067	3.80	3.80E-06	2950.00	2997.97	28.4502	27.29
4	2	11.27	0.0113	1.0290	0.0261	0.0131	0.2600	0.0066	3.70	3.70E-06	3045.95		26.1231	
5	4	11.14	0.0111	1.0245	0.0260	0.0130	0.2535	0.0064		3.42E-06	3253.05	3265.85	21.0998	20.79
6	4	11.25	0.0113	1.0225	0.0260	0.0130	0.2550	0.0065		3.43E-06	3278.64		20.4793	

Table 9A

Sintered Density and % Porosity of Al_2O_3 – Bronze Composite (10% Bronze; Sintering Temperature = 1500°C)

Sample Number	Sintering Time (Hrs.)	After Sintering Weight (gm)	Weight (kg)	Diameter (Inches)	Diameter (m)	Radius (m)	Thickness (Inches)	Thickness (m)	Volume (cm^3)	Volume (m^3)	Density (kg/m^3)	Average Density (kg/m^3)	Porosity (%)	Average Porosity (%)
1	0.5	11.38	0.0114	1.0275	0.0261	0.0130	0.2610	0.0066	3.70	3.70E-06	3075.68	2969.89	25.4020	27.97
2	0.5	11.17	0.0112	1.0235	0.0260	0.0130	0.2565	0.0065	3.90	3.90E-06	2864.10		30.5335	
3	2	11.12	0.0111	1.0205	0.0259	0.0130	0.2595	0.0066		3.48E-06	3197.05	3176.37	22.4582	22.96
4	2	11.03	0.0110	1.0230	0.0260	0.0130	0.2595	0.0066		3.50E-06	3155.69		23.4612	
5	4	10.94	0.0109	1.0245	0.0260	0.0130	0.2635	0.0067		3.56E-06	3073.41	3123.85	25.4569	24.23
6	4	10.86	0.0109	1.0200	0.0259	0.0130	0.2555	0.0065		3.42E-06	3174.29		23.0102	

Table 10A

Sintered Density and % Porosity of Al_2O_3 – Bronze Composite (20% Bronze; Sintering Temperature = 1300°C)

Sample Number	Sintering Time (Hrs.)	After Sintering Weight (gm)	Weight (kg)	Diameter (Inches)	Diameter (m)	Radius (m)	Thickness (Inches)	Thickness (m)	Volume (cm^3)	Volume (m^3)	Density (kg/m^3)	Average Density (kg/m^3)	Porosity (%)	Average Porosity (%)
1	0.5	11.13	0.0111	1.0835	0.0275	0.0138	0.2430	0.0062	3.60	3.60E-06	3091.67	3032.68	29.3172	30.67
2	0.5	11.30	0.0113	1.0520	0.0267	0.0134	0.2810	0.0071	3.80	3.80E-06	2973.68		32.0145	
3	2	10.87	0.0109	1.0705	0.0272	0.0136	0.2420	0.0061	3.60	3.60E-06	3019.44	3024.79	30.9683	30.85
4	2	11.06	0.0111	1.0665	0.0271	0.0135	0.2440	0.0062	3.65	3.65E-06	3030.14		30.7239	
5	4	11.07	0.0111	1.0650	0.0271	0.0135	0.2410	0.0061	3.65	3.65E-06	3032.88	3038.36	30.6613	30.54
6	4	11.11	0.0111	1.0755	0.0273	0.0137	0.2450	0.0062	3.65	3.65E-06	3043.84		30.4107	

Table 11A

Sintered Density and % Porosity of Al_2O_3 – Bronze Composite (20% Bronze; Sintering Temperature = 1400°C)

Sample	Sintering	After Sintering												
Number	Time (Hrs.)	Weight (gm)	Weight (kg)	Diameter (Inches)	Diameter (m)	Radius (m)	Thickness (Inches)	Thickness (m)	Volume (cm^3)	Volume (m^3)	Density (kg/m^3)	Average Density (kg/m^3)	Porosity (%)	Average Porosity (%)
1	0.5	11.47	0.0115	1.0685	0.0271	0.0136	0.2465	0.0063	3.8	3.80E-06	3018.42	2961.11	30.9917	32.30
2	0.5	11.47	0.0115	1.0520	0.0267	0.0134	0.2545	0.0065	3.95	3.95E-06	2903.80		33.6123	
3	2	11.23	0.0112	1.0325	0.0262	0.0131	0.2695	0.0068	3.60	3.60E-06	3119.44	3120.04	28.6821	28.67
4	2	11.28	0.0113	1.0285	0.0261	0.0131	0.2655	0.0067		3.61E-06	3120.64		28.6547	
5	4	10.81	0.0108	1.0685	0.0271	0.0136	0.2460	0.0062	3.65	3.65E-06	2961.64	2959.99	32.2898	32.33
6	4	10.65	0.0107	1.0680	0.0271	0.0136	0.2390	0.0061	3.60	3.60E-06	2958.33		32.3655	

Table 12A

Sintered Density and % Porosity of Al_2O_3 – Bronze Composite (20% Bronze; Sintering Temperature = 1500°C)

Sample	Sintering	After Sintering													
Number	Time (Hrs.)	Weight (gm)	Weight (kg)	Diameter (Inches)	Diameter (m)	Radius (m)	Thickness (Inches)	Thickness (m)	Volume (cm^3)	Volume (m^3)	Density (kg/m^3)	Average Density (kg/m^3)	Porosity (%)	Average Porosity (%)
1	0.5	11.60	0.0116	1.0640	0.0270	0.0135	0.2650	0.0067	3.90	3.90E-06	2974.36	3004.32	31.9991	31.31
2	0.5	10.62	0.0106	1.0365	0.0263	0.0132	0.2525	0.0064	3.50	3.50E-06	3034.29		30.6290	
3	2	10.79	0.0108	1.0515	0.0267	0.0134	0.2605	0.0066	3.70	3.70E-06	2916.22	2890.05	33.3284	33.93
4	2	10.31	0.0103	1.0635	0.0270	0.0135	0.2400	0.0061	3.60	3.60E-06	2863.89		34.5247	
5	4	10.08	0.0101	1.0575	0.0269	0.0134	0.2320	0.0059		3.34E-06	3018.70	2879.21	30.9854	34.17
6	4	10.00	0.0100	1.0665	0.0271	0.0135	0.2330	0.0059	3.65	3.65E-06	2739.73		37.3634	

Table 1B

Modulus of Rupture (MOR) and Cutting Rate of Al_2O_3 – Bronze Composite (0% Bronze; Sintering Temperature = 1300°C)

Number	Deflection Measured	Load(F) (lb)	Load(F) (N)	Radius(R) (m)	Radius(R) (mm)	MOR(σ) (Mpa)	Cutting Time (Sec)	Cutting Depth (Inches)	Cutting Depth (m)	Thickness (m)	Cutting Area (m^2)	Cutting Rate (m^2/s)
1	36	252	1121.40	0.0128	12.7699	2.3998						
2	34	238	1059.10	0.0128	12.7889	2.2564						
3	27	189	841.05	0.0129	12.8588	1.7628						
4	32	224	996.80	0.0125	12.5413	2.2520						
5	23	161	716.45	0.0125	12.5413	1.6186						
6				0.0126	12.5857		210	0.112	0.002844	0.0076	2.17E-05	1.03E-07
7	40	280	1246.00	0.0124	12.4397	2.8845						
8	34	238	1059.10	0.0124	12.4206	2.4631						
9	42	294	1308.30	0.0124	12.4143	3.0474						

Note. (σ = MOR (Modulus of Rupture) / Flexural Strength / Rupture Strength; F = Force in Newton; L = Spacing between the two supports on the test fixture = 14mm; R = Radius of the specimen; 1 Deflection measured on the 3 point bend test fixture = 7 lb Force; 1 lb = 4.45 N)

Table 2B

Modulus of Rupture (MOR) and Cutting Rate of Al_2O_3 – Bronze Composite (0% Bronze; Sintering Temperature = 1400°C)

Sample Number	Deflection Measured	Load(F) (lb)	Load(F) (N)	Radius(R) (m)	Radius(R) (mm)	MOR(σ) (Mpa)
1	36	252	1121.40	0.0122	12.1984	2.7532
2	38	266	1183.70	0.0122	12.1793	2.9198
3	39	273	1214.85	0.0122	12.1857	2.9919
4	28	196	872.20	0.0121	12.1095	2.1889
5	48	336	1495.20	0.0121	12.0904	3.7701
6	38	266	1183.70	0.0121	12.1031	2.9753
7	36	252	1121.40	0.0121	12.0650	2.8455
8	46	322	1432.90	0.0121	12.0587	3.6416
9	46	322	1432.90	0.0121	12.0587	3.6416

Note. (σ = MOR (Modulus of Rupture) / Flexural Strength / Rupture Strength; F = Force in Newton; L = Spacing between the two supports on the test fixture = 14mm; R = Radius of the specimen; 1 Deflection measured on the 3 point bend test fixture = 7 lb Force; 1 lb = 4.45 N)

Table 3B

Modulus of Rupture (MOR) and Cutting Rate of Al_2O_3 – Bronze Composite (0% Bronze; Sintering Temperature = 1500°C)

Sample Number	Deflection Measured	Load(F) (lb)	Load(F) (N)	Radius(R) (m)	Radius(R) (mm)	MOR(σ) (Mpa)
1	37	259	1152.55	0.0120	12.0015	2.9712
2	48	336	1495.20	0.0120	12.0015	3.8545
3	38	266	1183.70	0.0120	12.0015	3.0515
4	23	161	716.45	0.0120	12.0015	1.8470
5	32	224	996.80	0.0120	12.0015	2.5697
6	27	189	841.05	0.0120	12.0015	2.1682
7	55	385	1713.25	0.0120	12.0015	4.4166
8	45	315	1401.75	0.0120	12.0015	3.6136
9	42	294	1308.30	0.0120	12.0015	3.3727

Note. (σ = MOR (Modulus of Rupture) / Flexural Strength / Rupture Strength; F = Force in Newton; L = Spacing between the two supports on the test fixture = 14mm; R = Radius of the specimen; 1 Deflection measured on the 3 point bend test fixture = 7 lb Force; 1 lb = 4.45 N)

Table 4B

Modulus of Rupture (MOR) and Cutting Rate of Al_2O_3 – Bronze Composite (5% Bronze; Sintering Temperature = 1300°C)

Sample Number	Deflection Measured	Load(F) (lb)	Load(F) (N)	Radius(R) (m)	Radius(R) (mm)	MOR(σ) (Mpa)
1	15	105	467.25	0.0131	13.0810	0.9303
2	16	112	498.40	0.0131	13.0747	0.9937
3	21	147	654.15	0.0129	12.9350	1.3470
4	22	154	685.30	0.0129	12.9286	1.4132
5	20	140	623.00	0.0130	12.9604	1.2753
6	14	98	436.10	0.0129	12.9223	0.9006

Note. (σ = MOR (Modulus of Rupture) / Flexural Strength / Rupture Strength; F = Force in Newton; L = Spacing between the two supports on the test fixture = 14mm; R = Radius of the specimen; 1 Deflection measured on the 3 point bend test fixture = 7 lb Force; 1 lb = 4.45 N)

Table 5B

Modulus of Rupture (MOR) and Cutting Rate of Al_2O_3 – Bronze Composite (5% Bronze; Sintering Temperature = 1400°C)

Sample Number	Deflection Measured	Load(F) (lb)	Load(F) (N)	Radius(R) (m)	Radius(R) (mm)	MOR(σ) (Mpa)	Cutting Time (Sec)	Cutting Depth (Inches)	Cutting Depth (m)	Thickness (m)	Cutting Area (m^2)	Cutting Rate (m^2/s)
1							71	0.396	0.01006	0.0065	6.58E-05	9.27E-07
2	14	98	436.10	0.01290	12.9032	0.9046						
3	22	154	685.30	0.01287	12.8778	1.4300						
4	18	126	560.70	0.01288	12.8842	1.1683						
5							60	0.353	0.00897	0.0065	5.81E-05	9.68E-07
6	21	147	654.15	0.01287	12.8778	1.3650						

Note. (σ = MOR (Modulus of Rupture) / Flexural Strength / Rupture Strength; F = Force in Newton; L = Spacing between the two supports on the test fixture = 14mm; R = Radius of the specimen; 1 Deflection measured on the 3 point bend test fixture = 7 lb Force; 1 lb = 4.45 N)

Table 6B

Modulus of Rupture (MOR) and Cutting Rate of Al_2O_3 – Bronze Composite (5% Bronze; Sintering Temperature = 1500°C)

Sample Number	Deflection Measured	Load(F) (lb)	Load(F) (N)	Radius(R) (m)	Radius(R) (mm)	MOR(σ) (Mpa)	Cutting Time (Sec)	Cutting Depth (Inches)	Cutting Depth (m)	Thickness (m)	Cutting Area (m^2)	Cutting Rate (m^2/s)
1	25	175	778.75	0.0128	12.8270	1.6444						
2	26	182	809.90	0.0128	12.8461	1.7025						
3												
4							60	0.387	0.0098	0.0064	6.32E-05	1.05E-06
5							72	0.522	0.0133	0.0065	8.59E-05	1.19E-06
6	13	91	404.95	0.0128	12.7953	0.8615						

Note. (σ = MOR (Modulus of Rupture) / Flexural Strength / Rupture Strength; F = Force in Newton; L = Spacing between the two supports on the test fixture = 14mm; R = Radius of the specimen; 1 Deflection measured on the 3 point bend test fixture = 7 lb Force; 1 lb = 4.45 N)

Table 7B

Modulus of Rupture (MOR) and Cutting Rate of Al_2O_3 – Bronze Composite (10% Bronze; Sintering Temperature = 1300°C)

Sample Number	Deflection Measured	Load(F) (lb)	Load(F) (N)	Radius(R) (m)	Radius(R) (mm)	MOR(σ) (Mpa)	Cutting Time (Sec)	Cutting Depth (Inches)	Cutting Depth (m)	Thickness (m)	Cutting Area (m^2)	Cutting Rate (m^2/s)
1							120	0.342	0.0087	0.00715	6.21E-05	5.18E-07
2							170	0.439	0.0112	0.006756	7.53E-05	4.43E-07
3							60	0.111	0.0028	0.007379	2.08E-05	3.47E-07
4	15	105	467.25	0.0130	13.0000	0.9478						
5												
6							60	0.201	0.0051	0.006782	3.46E-05	5.77E-07

Note. (σ = MOR (Modulus of Rupture) / Flexural Strength / Rupture Strength; F = Force in Newton; L = Spacing between the two supports on the test fixture = 14mm; R = Radius of the specimen; 1 Deflection measured on the 3 point bend test fixture = 7 lb Force; 1 lb = 4.45 N)

Table 8B

Modulus of Rupture (MOR) and Cutting Rate of Al_2O_3 – Bronze Composite (10% Bronze; Sintering Temperature = 1400°C)

Sample Number	Deflection Measured	Load(F) (lb)	Load(F) (N)	Radius(R) (m)	Radius(R) (mm)	MOR(σ) (Mpa)	Cutting Time (Sec)	Cutting Depth (Inches)	Cutting Depth (m)	Thickness (m)	Cutting Area (m^2)	Cutting Rate (m^2/s)
1	23	161	716.45	0.0130	13.0239	1.4453						
2							92	0.392	0.00996	0.00669	6.66E-05	7.24E-07
3							66	0.261	0.00663	0.00667	4.42E-05	6.7E-07
4							85	0.314	0.00798	0.0066	5.27E-05	6.2E-07
5	16	112	498.40	0.0130	13.0112	1.0083						
6	17	119	529.55	0.0130	12.9858	1.0777						

Note. (σ = MOR (Modulus of Rupture) / Flexural Strength / Rupture Strength; F = Force in Newton; L = Spacing between the two supports on the test fixture = 14mm; R = Radius of the specimen; 1 Deflection measured on the 3 point bend test fixture = 7 lb Force; 1 lb = 4.45 N)

Table 9B

Modulus of Rupture (MOR) and Cutting Rate of Al_2O_3 – Bronze Composite (10% Bronze; Sintering Temperature = 1500°C)

Sample Number	Deflection Measured	Load(F) (lb)	Load(F) (N)	Radius(R) (m)	Radius(R) (mm)	MOR(σ) (Mpa)	Cutting Time (Sec)	Cutting Depth (Inches)	Cutting Depth (m)	Thickness (m)	Cutting Area (m^2)	Cutting Rate (m^2/s)
1							110	0.499	0.0127	0.00663	8.4E-05	7.64E-07
2							60	0.249	0.0063	0.00652	4.12E-05	6.87E-07
3	14	98	436.10	0.0130	12.9604	0.8927						
4	16	112	498.40	0.0130	12.9921	1.0128						
5	10	70	311.50	0.0130	13.0112	0.6302						
6	12	84	373.80	0.0130	12.9540	0.7663						

Note. (σ = MOR (Modulus of Rupture) / Flexural Strength / Rupture Strength; F = Force in Newton; L = Spacing between the two supports on the test fixture = 14mm; R = Radius of the specimen; 1 Deflection measured on the 3 point bend test fixture = 7 lb Force; 1 lb = 4.45 N)

Table 10B

Modulus of Rupture (MOR) and Cutting Rate of Al_2O_3 – Bronze Composite (20% Bronze; Sintering Temperature = 1300°C)

Number	Cutting Time (Sec)	Cutting Depth (Inches)	Cutting Depth (m)	Thickness (m)	Cutting Area (m^2)	Cutting Rate (m^2/s)
1	22	0.186	0.0047	0.0062	2.92E-05	1.33E-06
2	50	0.482	0.0122	0.0071	8.74E-05	1.75E-06
3	45	0.551	0.0140	0.0061	8.6E-05	1.91E-06
4	49	0.429	0.0109	0.0062	6.75E-05	1.38E-06
5	50	0.595	0.0151	0.0061	9.25E-05	1.85E-06
6	53	0.475	0.0121	0.0062	7.51E-05	1.42E-06

Table 11B

Modulus of Rupture (MOR) and Cutting Rate of Al_2O_3 – Bronze Composite (20% Bronze; Sintering Temperature = 1400°C)

Sample Number	Deflection Measured	Load(F) (lb)	Load(F) (N)	Radius(R) (m)	Radius(R) (mm)	MOR(σ) (Mpa)	Cutting Time (Sec)	Cutting Depth (Inches)	Cutting Depth (m)	Thickness (m)	Cutting Area (m^2)	Cutting Rate (m^2/s)
1							35	0.569	0.01445	0.0063	9.05E-05	2.59E-06
2							53	0.422	0.01072	0.0065	6.93E-05	1.31E-06
3							69	0.44	0.01118	0.0068	7.65E-05	1.11E-06
4	13	91	404.95	0.0131	13.0620	0.8098						
5							40	0.634	0.0161	0.0062	0.000101	2.52E-06
6							47	0.664	0.01687	0.0061	0.000102	2.18E-06

Note. (σ = MOR (Modulus of Rupture) / Flexural Strength / Rupture Strength; F = Force in Newton; L = Spacing between the two supports on the test fixture = 14mm; R = Radius of the specimen; 1 Deflection measured on the 3 point bend test fixture = 7 lb Force; 1 lb = 4.45 N)

Table 12B

Modulus of Rupture (MOR) and Cutting Rate of Al_2O_3 – Bronze Composite (20% Bronze; Sintering Temperature = 1500°C)

Sample Number	Deflection Measured	Load(F) (lb)	Load(F) (N)	Radius(R) (m)	Radius(R) (mm)	MOR(σ) (Mpa)	Cutting Time (Sec)	Cutting Depth (Inches)	Cutting Depth (m)	Thickness (m)	Cutting Area (m^2)	Cutting Rate (m^2/s)
1							35	0.507	0.01288	0.0067	8.67E-05	2.48E-06
2							50	0.562	0.01427	0.0064	9.16E-05	1.83E-06
3							40	0.618	0.0157	0.0066	0.000104	2.6E-06
4							33	0.647	0.01643	0.0061	0.0001	3.04E-06
5	10	70	311.50	0.0134	13.4303	0.5730						
6							28	0.763	0.01938	0.0059	0.000115	4.1E-06

Note. (σ = MOR (Modulus of Rupture) / Flexural Strength / Rupture Strength; F = Force in Newton; L = Spacing between the two supports on the test fixture = 14mm; R = Radius of the specimen; 1 Deflection measured on the 3 point bend test fixture = 7 lb Force; 1 lb = 4.45 N)

Table 13

Rule-of-Mixture (ROM) Density of Al_2O_3 – Bronze Composites

Weight fraction of bronze in the composite (Weight %)	Volume fraction of bronze in the composite (Volume %)	ROM density (kg/m^3)
0	0.00	3900
5	2.35	4008
10	4.83	4123
20	10.25	4374

Table 14

Sintered Density and %Bronze of Al_2O_3 – Bronze Composite (0.5hr, 2.0hr and 4.0hr; Sintering Temperature = 1300°C)

Al_2O_3 (% Bronze)	Time (Hrs.)	Temp (°C)	Density (kg/m^3)
0	0.5	1300	3191.09
5	0.5	1300	3025.13
10	0.5	1300	2866.80
20	0.5	1300	3032.68
0	2	1300	3507.40
5	2	1300	3169.08
10	2	1300	3053.54
20	2	1300	3024.79
0	4	1300	3497.11
5	4	1300	3206.46
10	4	1300	3354.10
20	4	1300	3038.35

Table 15

Sintered Density and %Bronze of Al_2O_3 – Bronze Composite (0.5hr, 2.0hr and 4.0hr; Sintering Temperature = 1400°C)

Al_2O_3 (% Bronze)	Time (Hrs.)	Temp (°C)	Density (kg/m^3)
0	0.5	1400	3683.25
5	0.5	1400	3372.53
10	0.5	1400	3183.71
20	0.5	1400	2961.10
0	2	1400	3747.55
5	2	1400	3177.57
10	2	1400	2997.97
20	2	1400	3120.04
0	4	1400	3792.71
5	4	1400	3269.52
10	4	1400	3265.84
20	4	1400	2959.98

Table 16

Sintered Density and %Bronze of Al_2O_3 – Bronze Composite (0.5hr, 2.0hr and 4.0hr; Sintering Temperature = 1500°C)

Al_2O_3 (% Bronze)	Time (Hrs.)	Temp (°C)	Density (kg/m^3)
0	0.5	1500	3885.06
5	0.5	1500	3249.77
10	0.5	1500	2969.88
20	0.5	1500	3004.32
0	2	1500	3861.52
5	2	1500	3576.27
10	2	1500	3176.37
20	2	1500	2890.05
0	4	1500	3842.36
5	4	1500	3327.35
10	4	1500	3123.85
20	4	1500	2879.21

Table 17

Sintering Temperature and Sintered Density of Al_2O_3 – Bronze Composite (0%, 5%, 10% and 20% Bronze; Sintering Time = 0.5hr)

Al_2O_3 (% Bronze)	Time (Hrs.)	Temp (°C)	Density (kg/m^3)
0	0.5	1300	3191.09
0	0.5	1400	3683.26
0	0.5	1500	3885.06
5	0.5	1300	3025.13
5	0.5	1400	3372.54
5	0.5	1500	3249.78
10	0.5	1300	2866.80
10	0.5	1400	3183.71
10	0.5	1500	2969.89
20	0.5	1300	3032.68
20	0.5	1400	2961.11
20	0.5	1500	3004.32

Table 18

Sintering Temperature and Sintered Density of Al_2O_3 – Bronze Composite (0%, 5%, 10% and 20% Bronze; Sintering Time = 2hr)

Al_2O_3 (% Bronze)	Time (Hrs.)	Temp (°C)	Density (kg/m^3)
0	2	1300	3507.40
0	2	1400	3747.55
0	2	1500	3861.52
5	2	1300	3169.07
5	2	1400	3177.57
5	2	1500	3576.27
10	2	1300	3053.54
10	2	1400	2997.97
10	2	1500	3176.37
20	2	1300	3024.79
20	2	1400	3120.04
20	2	1500	2890.05

Table 19

Sintering Temperature and Sintered Density of Al_2O_3 – Bronze Composite (0%, 5%, 10% and 20% Bronze; Sintering Time = 4hr)

Al_2O_3 (% Bronze)	Time (Hrs.)	Temp (°C)	Density (kg/m^3)
0	4	1300	3497.11
0	4	1400	3792.72
0	4	1500	3842.37
5	4	1300	3206.47
5	4	1400	3269.53
5	4	1500	3327.35
10	4	1300	3354.10
10	4	1400	3265.85
10	4	1500	3123.85
20	4	1300	3038.36
20	4	1400	2959.99
20	4	1500	2879.21

Table 20

Sintering Time and Sintered Density of Al_2O_3 – Bronze Composite (1300°C, 1400°C and 1500°C; Bronze = 0%)

Al_2O_3 (%Bronze)	Time (Hrs.)	Temp (°C)	Density (kg/m^3)
0	0.5	1300	3191.09
0	2	1300	3507.40
0	4	1300	3497.11
0	0.5	1400	3683.26
0	2	1400	3747.55
0	4	1400	3792.72
0	0.5	1500	3885.06
0	2	1500	3861.53
0	4	1500	3842.37

Table 21

Sintering Time and Sintered Density of Al_2O_3 – Bronze Composite (1300°C, 1400°C and 1500°C; Bronze = 5%)

Al_2O_3 (%Bronze)	Time (Hrs.)	Temp (°C)	Density (kg/m^3)
5	0.5	1300	3025.13
5	2	1300	3169.08
5	4	1300	3206.47
5	0.5	1400	3372.54
5	2	1400	3177.58
5	4	1400	3269.53
5	0.5	1500	3249.78
5	2	1500	3576.27
5	4	1500	3327.35

Table 22

Sintering Time and Sintered Density of Al_2O_3 – Bronze Composite (1300°C, 1400°C and 1500°C; Bronze = 10%)

Al_2O_3 (%Bronze)	Time (Hrs.)	Temp (°C)	Density (kg/m^3)
10	0.5	1300	2866.80
10	2	1300	3053.54
10	4	1300	3354.10
10	0.5	1400	3183.71
10	2	1400	2997.97
10	4	1400	3265.85
10	0.5	1500	2969.89
10	2	1500	3176.37
10	4	1500	3123.85

Table 23

Sintering Time and Sintered Density of Al_2O_3 – Bronze Composite (1300°C, 1400°C and 1500°C; Bronze = 20%)

Al_2O_3 (%Bronze)	Time (Hrs.)	Temp (°C)	Density (kg/m^3)
20	0.5	1300	3032.68
20	2	1300	3024.79
20	4	1300	3038.36
20	0.5	1400	2961.11
20	2	1400	3120.04
20	4	1400	2959.99
20	0.5	1500	3004.32
20	2	1500	2890.05
20	4	1500	2879.21

Table 24

Sintered Density, Porosity, MOR and Cutting Rate of Al_2O_3 – Bronze Composite with 0%, 5%, 10% and 20% Bronze under Sintering Temperatures 1300°C, 1400°C and 1500°C.

Sample Number	Al_2O_3 (%Bronze)	Temp (°C)	Density (kg/m^3)	Porosity (%)	MOR(σ) (MPa)	Cutting Rate (m^2/s)
1	0	1300	3225.98	17.2826	2.3998	
2	0	1300	3204.96	17.8216	2.2564	
3	0	1300	3142.35	19.4270	1.7628	
4	0	1300	3404.39	12.7080	2.2520	
5	0	1300	3364.48	13.7313	1.6186	
6	0	1300	3753.33	3.7607	[redacted]	1.03E-07
7	0	1300	3490.21	10.5075	2.8845	
8	0	1300	3492.53	10.4479	2.4631	
9	0	1300	3508.59	10.0361	3.0474	
10	0	1400	3666.03	5.9992	2.7532	
11	0	1400	3726.61	4.4458	2.9198	
12	0	1400	3657.13	6.2275	2.9919	
13	0	1400	3727.68	4.4184	2.1889	
14	0	1400	3777.60	3.1386	3.7701	
15	0	1400	3737.38	4.1698	2.9753	
16	0	1400	3789.41	2.8356	2.8455	
17	0	1400	3783.78	2.9800	3.6416	
18	0	1400	3804.97	2.4368	3.6416	
19	0	1500	3890.86	0.2342	2.9712	
20	0	1500	3863.02	0.9481	3.8545	
21	0	1500	3901.31	-0.0335	3.0515	
22	0	1500	3828.22	1.8405	1.8470	
23	0	1500	3857.57	1.0879	2.5697	
24	0	1500	3898.79	0.0309	2.1682	
25	0	1500	3822.01	1.9998	4.4166	
26	0	1500	3878.24	0.5579	3.6136	
27	0	1500	3826.86	1.8753	3.3727	
28	5	1300	3014.83	24.7798	0.9303	
29	5	1300	3035.44	24.2656	0.9937	
30	5	1300	3178.42	20.6981	1.3470	
31	5	1300	3159.74	21.1643	1.4132	
32	5	1300	3200.46	20.1481	1.2753	
33	5	1300	3212.48	19.8484	0.9006	
34	5	1400	3555.93	11.2791	[redacted]	9.27E-07
35	5	1400	3189.14	20.4306	0.9046	
36	5	1400	3204.04	20.0589	1.4300	
37	5	1400	3151.12	21.3793	1.1683	
38	5	1400	3331.25	16.8850	[redacted]	9.68E-07
39	5	1400	3207.80	19.9650	1.3650	

Table 24:

Continued

Sample Number	Al_2O_3 (%Bronze)	Temp (°C)	Density (kg/m^3)	Porosity (%)	MOR(σ) (MPa)	Cutting Rate (m^2/s)
40	5	1500	3244.50	19.0493	1.6444	
41	5	1500	3255.05	18.7862	1.7025	
42	5	1500	[redacted]	[redacted]	[redacted]	
43	5	1500	3576.27	10.7717	[redacted]	1.05E-06
44	5	1500	3483.33	13.0905	[redacted]	1.19E-06
45	5	1500	3171.37	20.8739	0.8615	
46	10	1300	2845.00	30.9968	[redacted]	5.18E-07
47	10	1300	2888.61	29.9392	[redacted]	4.43E-07
48	10	1300	2873.42	30.3076	[redacted]	3.47E-07
49	10	1300	3233.66	21.5701	0.9478	
50	10	1300	3780.00	8.3192	[redacted]	
51	10	1300	2928.21	28.9788	[redacted]	5.77E-07
52	10	1400	3141.71	23.8004	1.4453	
53	10	1400	3225.71	21.7629	[redacted]	7.24E-07
54	10	1400	2950.00	28.4502	[redacted]	6.7E-07
55	10	1400	3045.95	26.1231	[redacted]	6.2E-07
56	10	1400	3253.05	21.0998	1.0083	
57	10	1400	3278.64	20.4793	1.0777	
58	10	1500	3075.68	25.4020	[redacted]	7.64E-07
59	10	1500	2864.10	30.5335	[redacted]	6.87E-07
60	10	1500	3197.05	22.4582	0.8927	
61	10	1500	3155.69	23.4612	1.0128	
62	10	1500	3073.41	25.4569	0.6302	
63	10	1500	3174.29	23.0102	0.7663	
64	20	1300	3091.67	29.3172	[redacted]	1.33E-06
65	20	1300	2973.68	32.0145	[redacted]	1.75E-06
66	20	1300	3019.44	30.9683	[redacted]	1.91E-06
67	20	1300	3030.14	30.7239	[redacted]	1.38E-06
68	20	1300	3032.88	30.6613	[redacted]	1.85E-06
69	20	1300	3043.84	30.4107	[redacted]	1.42E-06
70	20	1400	3018.42	30.9917	[redacted]	2.59E-06
71	20	1400	2903.80	33.6123	[redacted]	1.31E-06
72	20	1400	3119.44	28.6821	[redacted]	1.11E-06
73	20	1400	3120.64	28.6547	0.8098	
74	20	1400	2961.64	32.2898	[redacted]	2.52E-06
75	20	1400	2958.33	32.3655	[redacted]	2.18E-06
76	20	1500	2974.36	31.9991	[redacted]	2.48E-06
77	20	1500	3034.29	30.6290	[redacted]	1.83E-06
78	20	1500	2916.22	33.3284	[redacted]	2.6E-06
79	20	1500	2863.89	34.5247	[redacted]	3.04E-06
80	20	1500	3018.70	30.9854	0.5730	
81	20	1500	2739.73	37.3634	[redacted]	4.1E-06

Figure 1

% Porosity and MOR

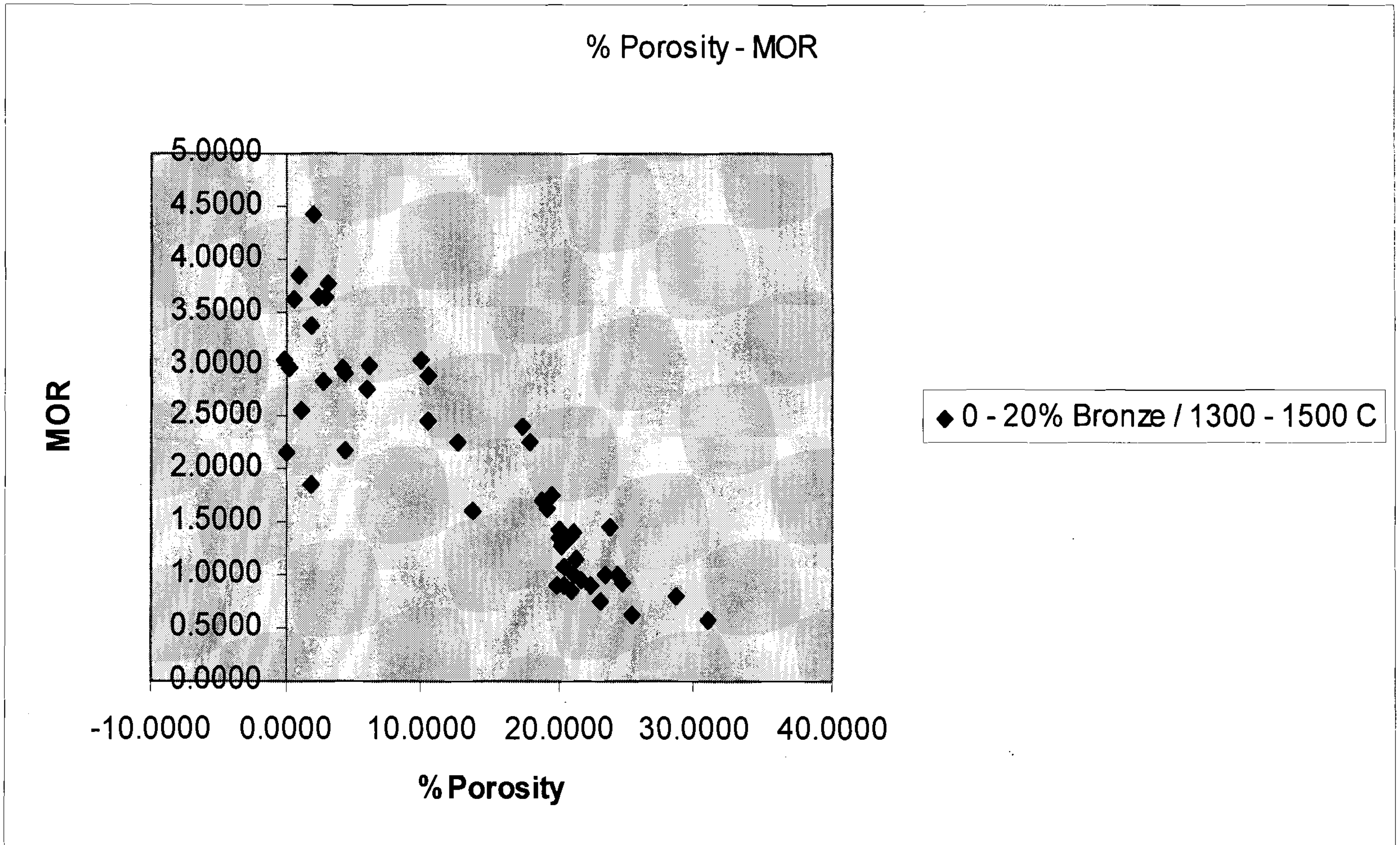

Figure 2

% Bronze - % Porosity

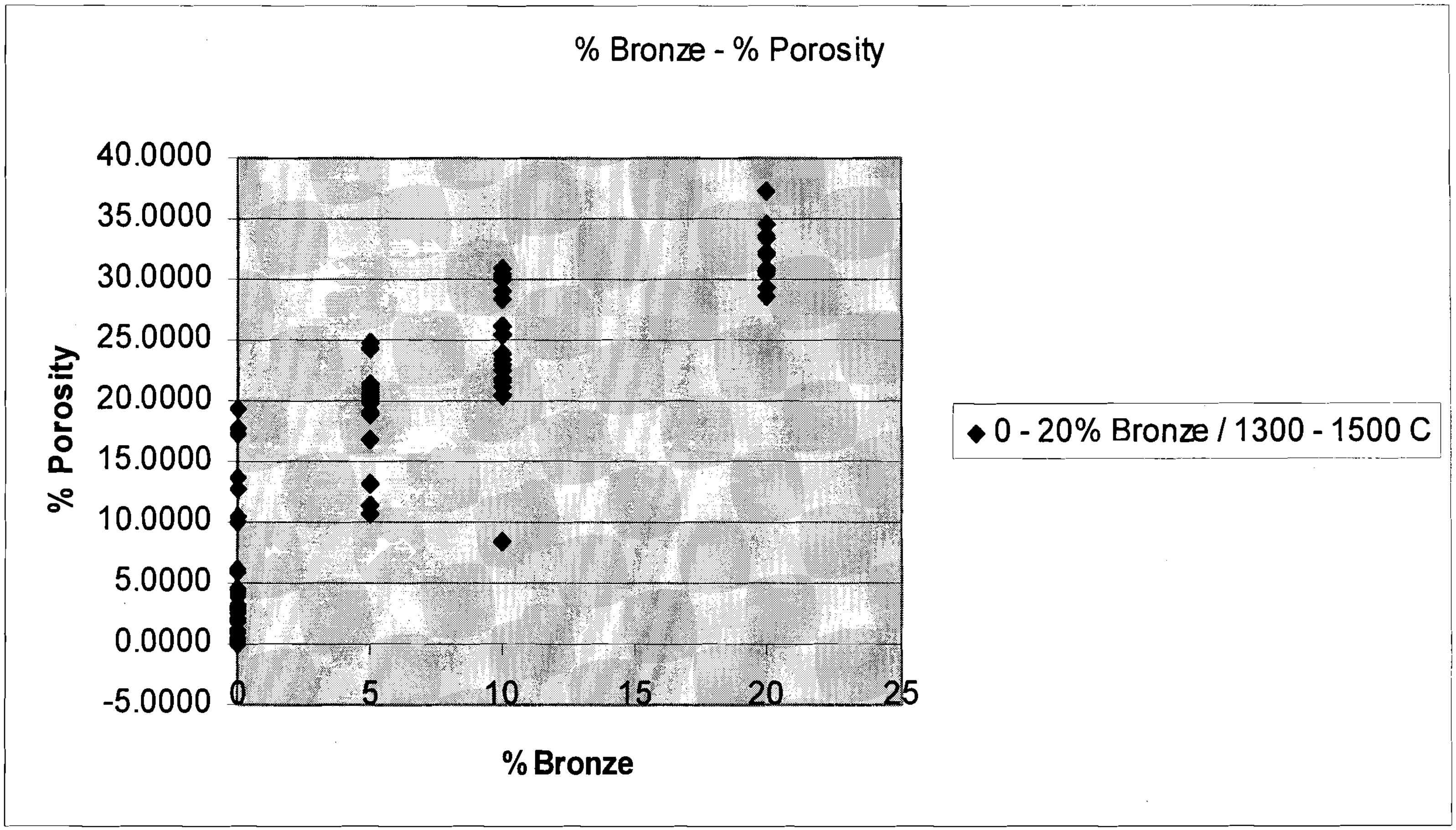

Figure 3

% Bronze and Cutting Rate

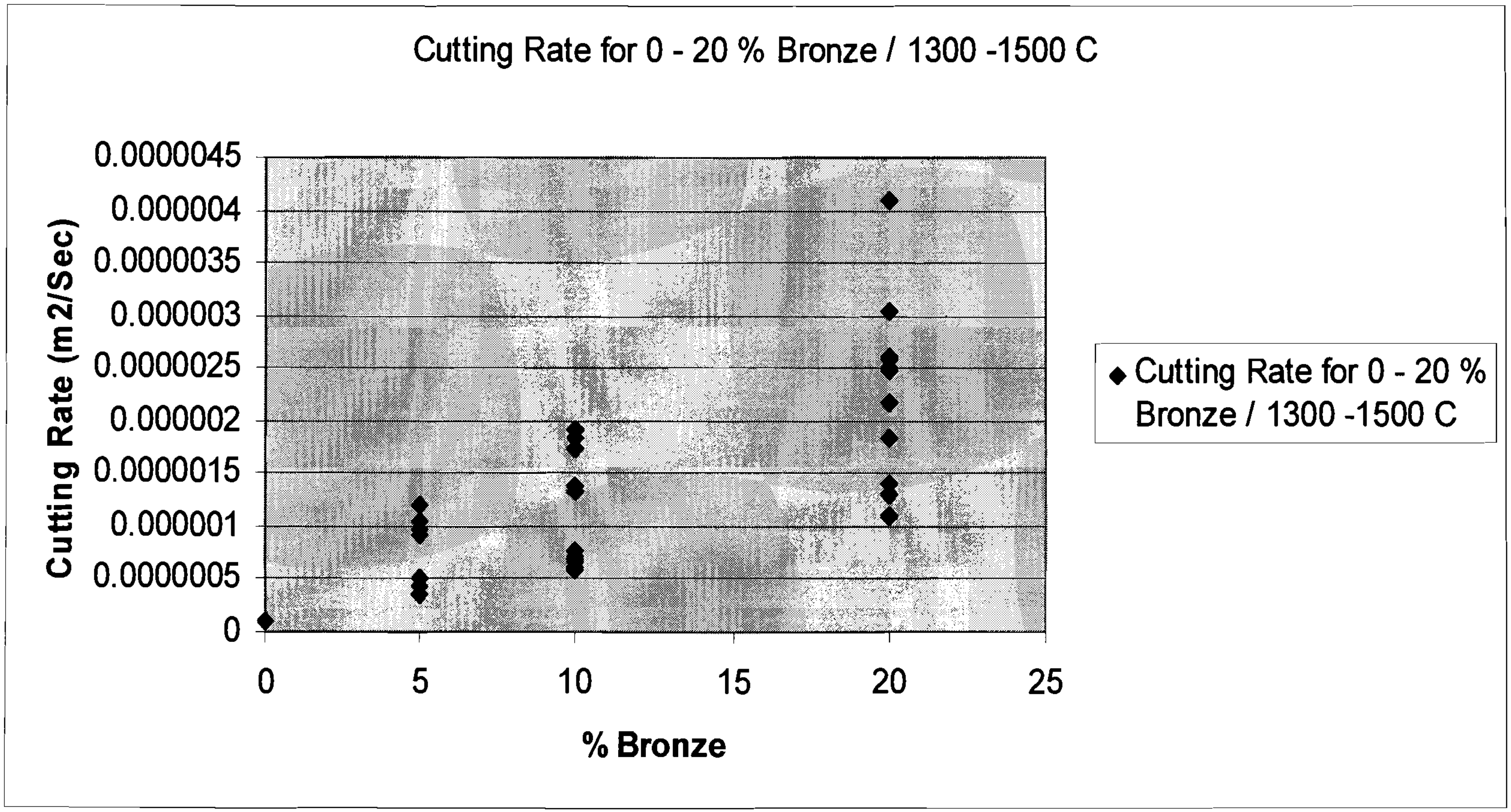

References

Asthana, R., Kumar, A., & Dahotre, N.B. (2006). *Materials Processing and Manufacturing Science*. Elsevier: Academic Press.

Beraud, C. M., Courbier, M., Esnouf, C., Juve, D., & Treheux, D. (1989). Study of copper-alumina bonding, *Journal of Materials Science, 24*(12), 4545-4554.

Chakladar, A. C. D., Armstrong, A. M., & Misra, S. K. (1968). Interface reactions between metals and ceramics: IV. Wetting of sapphire by liquid copper-oxygen alloys. *Journal of the American Ceramic Society, 51*(11), 630-634.

Chidambaram, P., Meir, A., & Edwards, G. R. (1996). The nature of interfacial phenomena at copper-titanium/alumina and copper-oxygen/alumina interfaces. *Materials Science & Engineering, A206*, 249-258.

Dong, S. R., Tu, J. P., & Zhang, X. B. (2001) An investigation of the sliding wear behavior of Cu-matrix composite reinforced by carbon nanotubes. *Materials Science and Engineering, A313*, 83-87.

Eustathopoulos, N., Chatain, D., & Coudurier, L. (1991). Wetting and interfacial chemistry in liquid metal ceramic systems. *Materials Science and Engineering, A135*, 83-88.

Ferkel, H., & Mordike, B. L. (2001). Magnesium strengthened by SiC nanoparticles. *Materials Science and Engineering, A298*, 193-199.

Frekel, H., & Riehemann, W. (1996). Bonding of alumina ceramics with nanoscaled alumina powders. *Nanostructured Materials, 7*(8), 835-845.

Kanetkar, C. S., Kacar, A. S., & Stefanescu, D. M. (1988). Wetting characteristics and surface tension of some Ni-base alloys on yttria, hafnia, alumina and zirconia substrates. *Metallurgical and Materials Transactions, 19A*, 1833-1839.

Kingery, W. D., Bowen, H. K., & Uhlmann, D. R. (1976). *Introduction to Ceramics.* New York : John Wiley & Sons Inc.

Locatelli, M. R., Tomsia, A. P., Nakashima, K., Dalgleish, B. J., & Glaser, A. M. (1995). New strategies for joining ceramics for high-temperature applications. *Key Engineering Materials, 111-112*, 157-190.

Mandal, S., Kumar, A., & Ray, A. K. (2004). Correlation between the mechanical properties and the microstructural behavior of Al_2O_3-(Ag-Cu-Ti) brazed joints. *Materials Science and Engineering, A383*, 235-244.

Mishra, P., Sengupta, P., Athavale, S. N., Pappachan, A. L, Grover, A. K., Suri, A. K., Kale, G. B., De, P. K., & Bhanumurthy, K. (2005). Brazing of hot isostatically pressed alumina-to-stainless steel (AISI 304L) by Mo-Mn route using 72Ag-28Cu braze. *Metallurgical and Materials Transactions, 36A*, 1487-1494.

Naka, M., & Hafez, K. M. (2003). Applying ultrasonic waves on brazing of alumina to copper using Zn-Al filler alloy. *Journal of Materials Science, 38*, 3491-3494.

Nicholas, M. G. (1988). Interactions at oxide-metal interfaces. *Materials Science Forum, 29*, 127-150.

Reed, J. S. (1988). *Principles of Ceramic Processing.* New York: John Wiley & Sons Inc.

Ritland, M. A., & Readey, D. W. (1993). Alumina-copper composites by vapor phase sintering. *Ceramic Engineering and Science Proceedings, 14*(9-10), 896-907.

Ritter, J. E., & Burton, M. S. (1967). Adherence and wettability of Ni, Ni-Ti, and Ni-Cr alloys to sapphire. *Transactions of the Metallurgical Society of AIME, 239*, 21-26.

Sekino, T., Yu, J. H., Choa, Y. H., & Niihara, K. (2000). Reduction and sintering of alumina/tungsten nanocomposites. *Journal of the Ceramic Society of Japan, 108*(6), 541-547.

Shalek, P. D., Petrovic, J. J., Hurley, G. F., & Gac, F. D. (1986). Hot-pressed SiC whisker/Si3N4 matrix composites. *American Ceramic Society Bulletin, 65*(2), 351-356.

Suganuma, K., Miyamoto, Y., & Koizumi, M. (1988). Joining of Ceramics and Metals. *Annual Review of Materials Science, 18*, 47-73.

Wei, G.C., & Becher, P. F. (1984). Improvements in mechanical properties in SiC by the addition of TiC Particles. *Journal of the American Ceramic Society, 67*(8), 571-574.

Wei, G.C., & Becher, P. F. (1985). Development of SiC-whisker-Reinforced ceramics. *Ceramic Bulletin, 64*(2), 298-304.

Xue, X. M., Wang, J. T., & Sui, Z. T. (1993). Wettability and interfacial reactions of alumina and zirconia by reactive Ag-In base alloy at mid-temperatures. *Journal of Materials Science, 28,* 1317-1322.

Ying, D. Y., & Zhang, D. L. (2000). Processing of Cu-Al2O3 metal matrix nanocomposite materials by using high energy ball milling. *Materials Science and Engineering, A286*, 152-156.

Zhang, J. X., Chandel, R. S., & Seow, H. P. (2002). Effect of chromium addition on brazing of copper to alumina: some microstructural aspects. *Science and Technology of Welding and Joining, 7*(3), 182-186.